

**EFFECT OF SINTERING TEMPERATURE ON PREPARATION OF  
Nd<sub>1.9</sub>Sr<sub>0.1</sub>NiO<sub>4-δ</sub> CATHODE MATERIAL FOR INTERMEDIATE TEMPERATURE  
SOLID OXIDE FUEL CELL APPLICATIONS**

**J. D. PUNDE**

Department of Physics, S. S. Girls' College, Gondia 441 601 India

---

**Abstract:** Intermediate temperature solid oxide fuel cell (IT-SOFC) cathode Nd<sub>1.9</sub>Sr<sub>0.1</sub>NiO<sub>4</sub> was prepared by combustion method & Sintered at different temperatures. It is mixed ionic-electronic conducting (MIEC) oxides and has K<sub>2</sub>NiF<sub>4</sub>-type structure. The prepared samples were characterized using X-ray powder diffraction (XRD), microhardness testing and four-probe dc conductivity. A close scrutiny of XRD reveals that the prepared solid solutions of cathode sintered at 1000 °C are single-phase and the d-values matches well with the standard JCPDS data corresponding to pure Nd<sub>2</sub>NiO<sub>4</sub> with small deviation. The dc conductivity results showed the conductivity is maximum for material sintered at 1000 °C and the transition from negative temperature coefficient to positive temperature coefficient, within the solid solubility region, is observed at 640 °C.

**Keywords:** Intermediate temperature solid oxide fuel cell, mixed ionic-electronic conductor (MIEC), combustion method, K<sub>2</sub>NiF<sub>4</sub>-type structure, cathode.

## I. INTRODUCTION

The electrochemical device, solid oxide fuel cells (SOFCs) produce electricity and heat directly from gaseous fuels through an oxidation process with high efficiency and low pollution. The operating temperature of SOFC is high (800 °C – 1000 °C). At this operating temperature, platinum and some other noble metals were used as the cathode materials. In this temperature region, the kinetics associated with cathode reaction are sufficiently rapid that cell losses are relatively less. However, platinum is expensive and its compatibility with

the electrolyte is not so good [1]. Also, low-cost interconnect materials are not useful. To overcome above issues with SOFCs, many researchers are focus their work to reduce operating temperature and develop intermediate temperature solid oxide fuel cells (IT-SOFCs) which can operate in the range 500°C – 800°C.

Reducing the operating temperature with sufficient power output and durability appears to be the challenge of IT-SOFCs. Again, the two main problems have been identified: one the low ionic conductivity of electrolytes and other the high polarization resistance of the cathode. Researchers proposed various solutions on it. One of them consists in reducing the thickness of the electrolyte in order to decrease its ohmic drop at low temperature. An electrolyte film of some tens of micrometers that should be gas tight can be used. Concerning the cathode material, using a mixed ionic and electronic conducting material appears to be a promising way to transform the triple-phase boundary (TPB) into a double contact (mixed conductor/gas phase), thus, lowering the cathode polarization [2].

In past, less expensive perovskites, which possess the required properties for cathode material, attracted much interest. Particularly, composite cathodes consisting of strontium-doped lanthanum manganite (LSM) / YSZ have been used to increase the triple phase boundary (TPB) length. But it is worth mention here that LSM, is unsuitable for IT-SOFCs operating below 800°C. Due to its negligible ionic conductivity of LSM cathode, its electrochemical activities are poor, therefore an electrochemical reaction is strictly limited to the TPB [3].

In this row,  $Ba_{0.5}Sr_{0.5}Co_{0.8}Fe_{0.2}O_{3-\delta}$  (BSCF) perovskite oxides are also identified as one of the potential cathode materials for IT-SOFC. Zhou et al reviewed and emphasized on the understanding and optimization of BSCF-based cathode materials for IT-SOFCs [4]. The doubts about this material are related to its long term applications due to their high thermal expansion coefficients (TECs), low chemical stability because of their flexible redox behavior, as well as the high cost of compositional elements. Thus, recently more studies are going on development of a number of oxides materials for IT-SOFC cathode applications are directed for improved performance at their operating temperature high resistance to degradation during operation [5]. An important class of candidate materials for the next generation IT-SOFC cathodes belong to the perovskite related Ruddlesden-Popper (RP) series of layered oxides (formula  $A_{n+1}B_nO_{3n+1}$ ). They exhibit good electrochemical, catalytic

and electrical properties as well as thermal and mechanical stability [5]. A number of studies shows that the cathode materials having  $K_2NiF_4$ -type structure, first members of the RP series (for  $n = 1$ ,  $A_2BO_4$ ) are most demanding for IT-SOFC.

Thus, the present study focuses on preparation on the  $MIECK_2NiF_4$ -type structure  $Nd_{1.9}Sr_{0.1}NiO_{4+\delta}$  by combustion technique and sintered on different temperatures. The prepared samples were characterized using X-ray powder diffraction (XRD), micro-hardness testing, Fourier Transform Infrared Spectroscopy (FTIR) and four-probe dc conductivity.

## II. Experimental

The initial reagents neodymium acetate, strontium acetate and nickel acetate, used were procured from Aldrich Chemicals (USA) with purity > 99.9 %. All these reagents were dried at 120°C for 24 h in order to remove the traces of moisture present. The respective requisite reagents in stoichiometric ratio were dissolved in the double distilled deionised water separately and then mixed together in a single corning flask. The homogeneous aqueous solution was then heated by using hot plate. The residue obtained was then pulverized to get them in the form of powders. The pellets of diameter and thickness 13 mm and 1-2 mm, respectively, were obtained by uniaxially compressing ground powder at 3 tons  $cm^{-2}$  pressure with the help of Specac (UK) stainless steel die-punch and hydraulic press. The resulting pellets were initially calcined at 700 °C for 4 h in an electric furnace. Subsequently, they were crushed to obtained fine powder and re-pelletized of diameter and thickness 9 mm and 1-2 mm, respectively. The pellets were finally sintered at 1000°C for 4 h and allowed to cool in the furnace to room temperature.

The prepared sample was subjected to structural characterization by X-ray powder diffraction (XRD) with a PANalytical X'pert PRO (Philips, the Netherlands) instrument that employed  $CuK_{\alpha}$  radiation. A curved graphite crystal was used as a monochromator. The X-ray diffraction measurement were carried out in a  $2\Theta$  range from 10 to 80° with a step size and time per step of 0.020° and 5 s, respectively. The crystallite size of composition under study is 242.5 determined using X'pert Highscore plus software based on the following expression:

$$C_s = \frac{0.9\lambda}{\beta \cos\theta_B} \quad (1)$$

where  $C_s, \lambda$ , and  $\theta_B$  are thickness of crystallite, X-ray wavelength and Bragg's angle, respectively. Here,  $\beta$  was determined by:

$$\beta^2 = \beta_m^2 - \beta_s^2 \quad (2)$$

where,  $\beta_m$  and  $\beta_s$  were the measured and the standard full width of half maxima, FWHM, of diffracted line, respectively. The  $\beta_s$  was estimated from the XRD pattern obtained by running the experiment on a standard silicon sample provided by PANalytical, Netherlands. The IR spectra were recorded by ECO-ATR Fourier transform instrument. The spectra of powder sample were recorded in the region 4000 - 600  $\text{cm}^{-1}$ . The sintered densities of the sample were determined using Archimedes' principle with the help of Mettler XS105 dual range monopan balance with density kit attachment and built in density measurement software. The micro-hardness of the sample was measured by the Vickers indentation technique (HMV2 Series Shimadzu micro Hardness Tester, Japan).

A thin platinum film on both flat surfaces of the sintered pellet was obtained by d.c. sputtering and resulted in good ohmic contacts for d.c. electrical conductivity measurements. Prior to the conductivity measurement, the sample was spring-loaded in a ceramic cell holder (Amel, Italy) and heated to 700°C for 1 h to homogenize the charge carriers. The resistance during the cooling cycle was measured as a function of temperature using the four-probe method with a computer-controlled Keithley 6221 current source and a 2182A nanovoltmeter in delta mode. The temperature of the sample during the measurement was controlled with an accuracy of  $\pm 1$  K with a Eurotherm 2216e temperature controller. The tip of a calibrated thermocouple was kept in the vicinity of the sample to measure its actual temperature.

### **III. RESULT AND DISCUSSION**

#### ***X-ray powder diffraction***

The X-ray powder diffraction patterns of  $\text{Nd}_{1.9}\text{Sr}_{0.1}\text{NiO}_{4+\delta}$  sintered at 900°C (MACS-9), 1000°C (MACS-10) and 1100°C (MACS-11) for 4 h are shown in Fig.1(a), (b) and (c) respectively. The obtained XRD data were initially profile fitted using Highscore plus software and then indexed. In addition to the lines due to  $\text{Nd}_2\text{O}_3$  and SrO, the characteristic

diffracted lines due to initial reagents are clearly seen in Fig. 1 (a). On the other hand, Fig. 1 (b) and (c) reveals close matching of all the characteristics diffracted peaks with the JCPDS (joint committee for powder diffraction standard) data (File No. 01-080-2323) due to pure tetragonal  $\text{Nd}_2\text{NiO}_4$ . Absence of diffracted peak(s) corresponding to either reagents or any intermediate compound(s) confirms the formation of a single-phase tetragonal  $\text{Nd}_{1.9}\text{Sr}_{0.1}\text{NiO}_{4+\delta}$  solid solution. In order to ascertain the formation of solid solution and its consequence on host lattice structure, the lattice cell constants of materials under study were determined using Unitcell, a computer software [6].

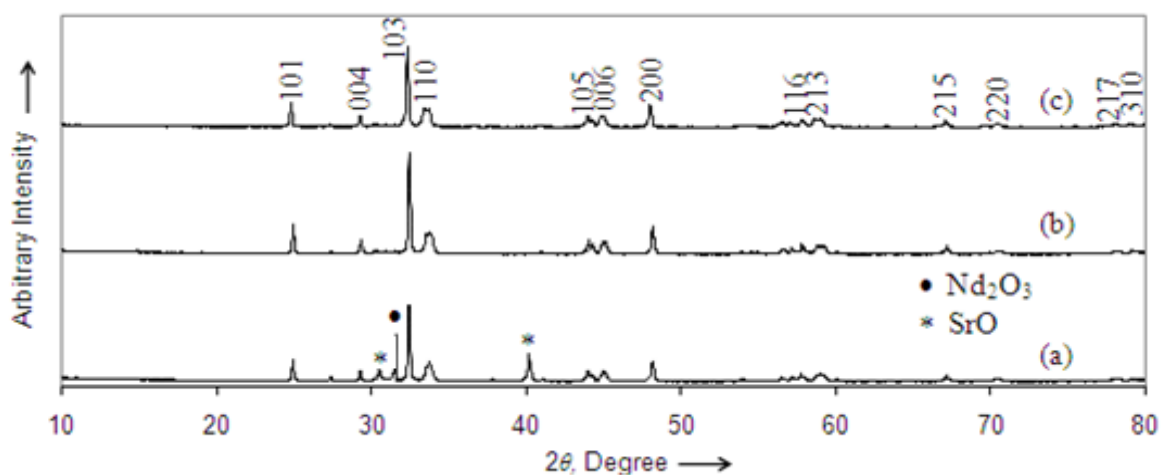


**Fig.1: The XRD patterns of  $\text{Nd}_{1.9}\text{Sr}_{0.1}\text{NiO}_{4+\delta}$  sintered at (a) 900°C (b) 1000°C and (c) 1100°C**

A comparison of lattice cell constants for  $\text{Nd}_{1.9}\text{Sr}_{0.1}\text{NiO}_{4+\delta}$  solid solution prepared by sintering combustion powder at three different temperatures is given in Table 1. It is seen that the lattice cell constant  $c$  and  $a$  remains almost unchanged on Sr addition compared to those of stoichiometric compound  $\text{Nd}_2\text{NiO}_4$  ( $a = 0.3854$  nm and  $c = 1.2140$  nm) [7]. Interestingly, as expected, the lattice cell constants do not change with change in sintering temperature. In contrast, the crystallite size increases significantly with an increase in sintering temperature, which is in line with the general observations. Since the single phase  $\text{Nd}_{1.9}\text{Sr}_{0.1}\text{NiO}_{4+\delta}$  forms on sintering the combustion powder even at 1000°C.

**Table 1:** A comparison of lattice cell constants ( $a$ ,  $c$  and  $v$ ), crystallite size ( $C_s$ ) and crystal lattice strain ( $S_l$ ) of  $Nd_{1.9}Sr_{0.1}NiO_{4+\delta}$  sintered at 900°C, 1000°C and 1100°C.

Composition	Code	$a$ (nm)	$c$ (nm)	$v$ (nm <sup>3</sup> )	$C_s$ (nm)	$S_l$ (%)
JCPDS		0.3854	1.214	--	-	--
$Nd_{1.9}Sr_{0.1}NiO_{4+\delta}$	NSNO-0.1 (MACS-9)	0.381	1.222	0.1801	201.3	0.16
$Nd_{1.9}Sr_{0.1}NiO_{4+\delta}$	NSNO-0.1 (MACS-10)	0.381	1.224	0.179	247.3	0.16
$Nd_{1.9}Sr_{0.1}NiO_{4+\delta}$	NSNO-0.1 (MACS-11)	0.381	1.225	0.1769	298.5	0.17

### Sinter density and microhardness number

The sintered density ( $\rho$ ) of the  $Nd_{1.9}Sr_{0.1}NiO_{4+\delta}$  prepared by combustion method and then sintered at 900, 1000 and 1100 °C, determined using the Archimedes principle, is compared in Table 2. A close look at the table reveals that the sintered density, increases with increased temperature. Also, the hardness number ( $HV$ ) increases and decreases commensurably. Such distinction is due to smaller grain size for material sintered at 1000°C (Table 2).

**Table 2:** Comparison of sinter density ( $\rho$ ) and microhardness number ( $HV$ ) of  $Nd_{1.9}Sr_{0.1}NiO_{4+\delta}$  sintered at 900, 1000 and 1100°C.

Sample code	$C_s$ (nm)	$\rho$ (%)	$a) HV$
NSNO-0.1 (MACS-9)	201.3	80±3	118
NSNO-0.1 (MACS-10)	247.3	81±1	125
NSNO-0.1 (MACS-11)	298.5	83±1	132

### Fourier Transform Infrared Spectroscopy (FTIR)

Fourier Transform Infrared Spectroscopy (FTIR) spectra of  $Nd_{1.9}Sr_{0.1}NiO_{4+\delta}$  sintered at 1000 °C in the region 4000 - 400 cm<sup>-1</sup> is shown in Fig. 2. A close look at the figures reveals presence of broad absorption peaks in the region 3500-2200 cm<sup>-1</sup> for the given sample. The

absorption band at the region  $700\text{-}600\text{ cm}^{-1}$  and  $500\text{-}400\text{ cm}^{-1}$  prove the material have  $K_2NiF_4$  - type  $A_2BO_4$  structure [8, 9]. The FTIR spectra of the sample of mixed oxides show weak absorption at  $700\text{-}400\text{ cm}^{-1}$ , which indicates that the  $Nd_{1.9}Sr_{0.1}NiO_{4+\delta}$  structure becomes microstrained and the microstrain of the coordination polyhedra depends on Ni. A low microstrain density does not change the original structure [10].

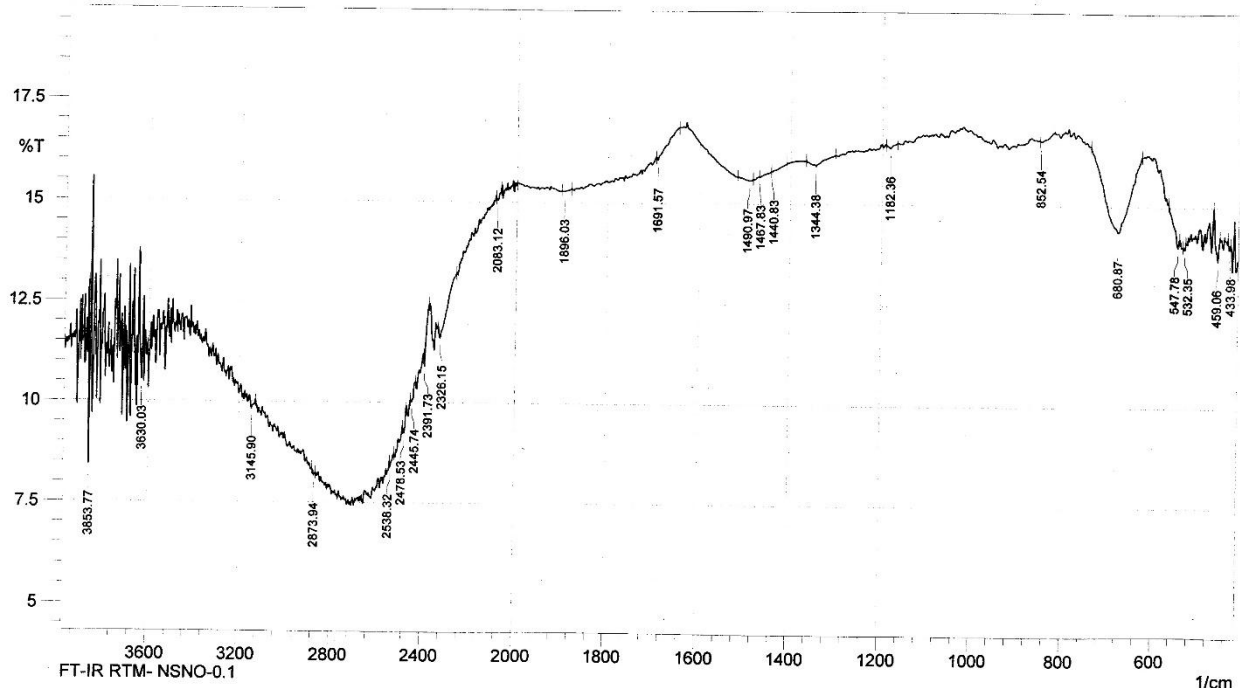


Fig. 2: FTIR spectra of  $Nd_{1.9}Sr_{0.9}NiO_{4+\delta}$

### dc conductivity

The temperature dependent dc conductivity of  $Nd_{1.9}Sr_{0.1}NiO_{4+\delta}$  sintered at 1000 and 1100°C is shown in Fig. 3. Both the samples exhibited positive temperature coefficient (PTC) of conductivity to negative temperature coefficient (NTC) transition at about 640°C. Such transition has been better explained by the defect chemistry [11, 12JD]. Furthermore, the conductivity is higher for the sample sintered at 1000°C than that for sintered at 1100°C. Below the transition temperature both the samples obey Arrhenius law given below,

$$\sigma T = (\sigma T)_0 \exp\left(\frac{-E_a}{kT}\right),$$

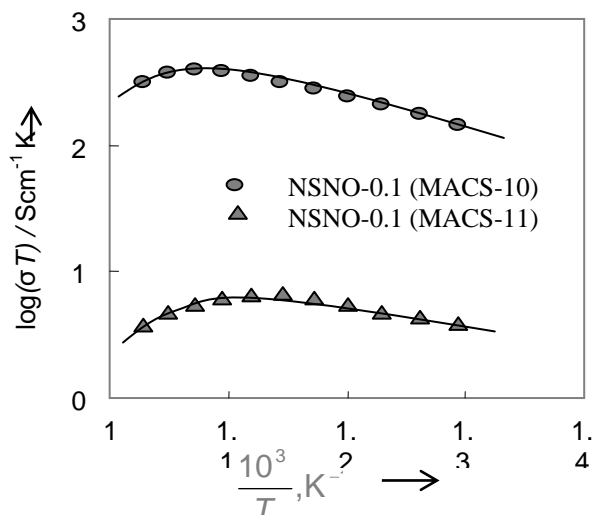


Fig. 3: Arrhenius plots for NSNO-0.1(MACS-10) and NSNO-0.1(MACS-11).

Where  $(\sigma T)_0$ ,  $k$ ,  $T$  and  $E_a$  are pre-exponential factor, Boltzmann constant, absolute temperature and activation energy, respectively. At higher temperatures ( $>640^\circ\text{C}$ ), however,  $\text{Nd}_{1.9}\text{Sr}_{0.1}\text{NiO}_{4+\delta}$  solid solutions lose some oxygen [13]. Concurrently, correlatively decreased charge holes carrier density that eventually reduced the dc conductivity above  $640^\circ\text{C}$ .

#### IV. CONCLUSIONS

The  $\text{Nd}_{1.9}\text{Sr}_{0.1}\text{NiO}_{4+\delta}$  solid solution prepared by combustion synthesis and sintered at  $900$ ,  $1000$  and  $1100^\circ\text{C}$ . XRD study confirms that there are lines due to initial reagents when sample sintered at  $900^\circ\text{C}$ . It also confirms the formation of single phase  $\text{Nd}_{1.9}\text{Sr}_{0.1}\text{NiO}_{4+\delta}$  at  $1000^\circ\text{C}$  and above. The sample under study is crystallizing with the tetragonal  $K_2\text{NiF}_4$ - type structure. The FTIR study indicates that the  $\text{Nd}_{1.9}\text{Sr}_{0.1}\text{NiO}_{4+\delta}$  structure becomes microstrained and the microstrain of the coordination polyhedra depends on Ni. Temperature dependent dc conductivity exhibits positive temperature coefficient to negative temperature coefficient transition at about  $640^\circ\text{C}$ . Therefore, for IT-SOFC cathode Sr doped  $\text{NdNiO}_4$  can be prepared by combustion synthesis and sintered at  $1000^\circ\text{C}$ .



## V. ACKNOWLEDGEMENTS

The authors are thankful to Materials Science Research Laboratory, Department of Physics, RTM, Nagpur University, Nagpur.

## VI. REFERENCES

1. J. M. Ralph, A. C. Schoeler, M. Krumpelt, *J. Mater. Sci.* 36 (2001) 1161–1172.
2. Joseph D. Fehribachand Ryan O'hayresiam, *J. Appl. Math*, Vol. 70, No. 2, pp. 510–530.
3. E. P. Murray, T. Tsai, S. A. Barnett, *Solid State Ionics* 110 (1998) 235, E. P. Murray, S. A. Barnett, *Solid State Ionics* 143 (2001) 265.
4. W. Zhou, R. Ran, Z. Shao, *J. Power Sources* 192 (2009) 231.
5. A. Chroneos, R. V. Vovk, I. L. Goulatis., L. I. Goulatis, *J. Alloys Compd.*doi: 10.1016/j.jallcom. 2010.01.071.
6. T. J. B. Holland, S. A. T. Redfern, *Mineral Mag.* 61 (1997) 65-67.
7. Joint committee for powder diffraction standard (JCPDS) data file no. 01-080-2323.
8. Xiaomao Yang, Laitao Luo, Hua Zhong, *Applied Catalysis A: General* 272 (2004) 299–303.
9. H. Lou, J. Liu, X. Liu, F. Ma, *J. Chin. Rare Earth Soc.* 19 (2001) 324.
10. H. Zhong, R. Zeng, *J. Serb. Chem. Soc.* 71 (10) (2006) 1049–1059.
11. E. Bohem, J.M. Basat, M.C. Steil, P. Dordor, F. Mauvy, J.C. Grenier, *Solid State Sciences* 5 (2003) 973-981.
12. A. P. Khandale, J. D. Punde, S. S. Bhoga, *J Solid State Electrochem* (2013) 17:617–626.
13. V.V. Washook, I.I. Yushkevich, L.V. Kokhonovsky, L.V. Makhonovsky, L.V. Makhanch, S.P. Tolochko, I.F. Kononyuk, H. Ullmann, H. Altenburg, *Solid State Ionics* 119 (1999) 23-30.